Biosensors and Bioelectronics 24 (2008) 951–957

Contents lists available at ScienceDirect

Biosensors and Bioelectronics

journal homepage: www.elsevier.com/locate/bios

A sensitive NADH and glucose biosensor tuned by visible light based on thionine bridged carbon nanotubes and gold nanoparticles multilayer

Liu Deng, Yizhe Wang, Li Shang, Dan Wen, Fuan Wang, Shaojun Dong*

State Key Laboratory of Electroanalytical Chemistry, Changchun Institute of Applied Chemistry, Chinese Academy of Sciences, Changchun, Number 5625, Renmin Road, Jilin 130022, PR China

ARTICLE INFO

Article history:
Received 24 April 2008
Received in revised form 7 July 2008
Accepted 25 July 2008
Available online 8 August 2008

Keywords:
Glucose dehydrogenase
NADH
Biosensor
Multiwalled carbon nanotube
Thionine
Gold nanoparticles

ABSTRACT

A NADH and glucose biosensor based on thionine cross-linked multiwalled carbon nanotubes (MWNTs) and Au nanoparticles (Au NPs) multilayer functionalized indium-doped tin oxide (ITO) electrode were presented in this paper. The effect of light irradiation on the enhancement of bioelectrocatalytic processes of the biocatalytic systems by the photovoltaic effect was investigated. This bioelectrode exhibited excellent catalytic activity of the oxidation towards dihydronicotinamide adenine dinucleotide (NADH). Most interesting, the performance of this NADH sensor could be tuned by the visible light. When the biosensor was performed in the dark, the anodic current increased linearly with NADH concentration over the range from 0.5 to 237 μM with detection limit 0.1 μM and sensitivity 17 nA μM^{-1}. The sensitivity became 115 nA μM^{-1} with detection limit 0.05 μM with the light irradiation. Compared with the reaction in dark, the sensitivity increased around 7 folds while the detection limit decreased 2 folds. The glucose biosensor also exhibited the same behavior. The linear range was from 10 μM to 2.56 mM with the sensitivity of 7.8 μA mM^{-1} and detection limit 5.0 μM in the dark. After the light irradiation, the linear range was from 1 μM to 3.25 mM with the sensitivity of 18.5 μA mM^{-1} and detection limit 0.7 μM. It indicated a potential to provide an operational access to develop new kinds of photocontrolled dehydrogenase enzyme-based bioelectronics.

1. Introduction

Dihydronicotinamide adenine dinucleotide (NADH) coenzyme oxidation at the electrode surface has received considerable interest due to its significance both as a cofactor for dehydrogenase enzymes and its role in the electron-transfer chain in biological system, and also due to the developing NADH-dependent dehydrogenases-based amperometric biosensors (Maleki et al., 2006). However, direct oxidation of NADH at bare electrode occurs at high overpotential (0.6–0.8 V) and suffers from low sensitivity and the fouling of the electrode surface by its oxidation products (Deore and Freund, 2005). In recent years, nanomaterials are attracting growing attention in facilitating electron transfer kinetics. Many nanomaterials, such as poly(1,2-diaminobenzene) nanotubules (Valentini et al., 2004), and TiO_2 nanostructured films (Curulli et al., 2005), particularly carbon nanotubes (CNTs) (Wang and Musameh, 2003; Tsai et al., 2007; Zhang et al., 2003; Zhang and Gorski, 2005), carbon nanofibers (CNFs) (Wu et al., 2007a,b; Arvinte et al., 2007) and gold nanoparticles (AuNPs) (Jena and Raj, 2006) have been devoted to decreasing the high overpotential for NADH oxidation and minimizing surface fouling. The ideal biosensor fabrication method should employ mild chemical conditions, allow for large quantities of enzyme to be immobilized, provide a favorable microenvironment to maintain the enzyme activity, and provide a large surface area for enzyme–substrate contact within a small total volume. Barriers to mass transport of substrate and product should be minimized, and a chemically and mechanically robust system should be provided. The unique electronic, chemical, mechanical properties and biocompatibility of CNTs and AuNPs suggest that AuNPs-functionalized MWCNTs may satisfies all of above criteria. In recent year, nanoparticles (NPs)/CNTs multilayer films have been assembled by LBL technique. Most multilayer structures are cross-linked by polyelectrolyte such as poly(dimethyldiallylammonium chloride) (Liu et al., 2007), chitosan (Ou et al., 2007), poly(ethyleneimine) (Yu et al., 2006), poly(sodium-*p*-styrenesulfonate) salt (Yang et al., 2006) and surfactant (Zhang et al., 2006) or via covalent-bonding interaction (Ma et al., 2008).

In this paper, we described the fabrication of CNTs/thionine/AuNPs self-assembled multilayers on amino functionalized surfaces by using thionine as cross-linkers. Here, CNTs/AuNPs

* Corresponding author. Tel.: +86 431 85262101; fax: +86 431 85689711.
E-mail address: dongsj@ciac.jl.cn (S. Dong).

0956-5663/$ – see front matter © 2008 Elsevier B.V. All rights reserved.
doi:10.1016/j.bios.2008.07.066

multilayer provided a suitable microenvironment to retain the enzyme activity and amplified the electrochemical signal of the product of the enzymatic reaction. Thionine has been successfully applied to fabricate AuNPs functional CNTs nanomaterial (Wang et al., 2007a), AuNPs multilayer (Chen et al., 2002) and CNTs multilayer (Huang et al., 2005) as cross-linker. But the effect of the light irradiation on the catalytic performance of those nanostructures has not yet been investigated, since the thionine is a photoactive molecular. There are several reports on the catalytic activity of the enzyme would affected through the tunable characteristic of the specific component in the matrix. The catalytic activity of the hemoglobin, which entrapped in the TiO_2 NPs can be tuned by the photovoltaic effect of TiO_2 induced by the ultraviolet light (Zhou et al., 2005). The effect of a constant magnetic field on the enhancement of bioelectrocatalytic processes of the surface-integrated biocatalytic systems by the magnetohydrodynamic effect is applied in the enhancement of the biofuel cell performance (Katz et al., 2005). So that we assumed that the performance of this NADH and glucose biosensor based on thionine bridged multilayer could be adjusted by the light irradiation, since the light would modulate the different state of the thionine in this multilayer structure. In the present paper, we reported a NADH and glucose biosensor based on the photoactive thionine into CNTs and AuNPs multilayer nanostructure, which performance could be reversibly switched between "low" and "high" states by the visible light irradiation. This self-assembly nanostructure allowed the efficient oxidation to NADH in the dark, and the electrode exhibited much better biocatalytic performance after the dye was activated by light. The activation and inhibition of the photovoltaic effect of the thionine by interval light irradiation provided a means to reversibly tune the photochemical process. This multicomponent nanostructure enabled the light-induced enhancement and photoswitchable biosensor to be constructed. Glucose dehydrogenase (GDH) was used as a model enzyme that can be simply immobilized on the electrode surface by adsorption process. A sensitive amperometric sensor for the glucose with low potential and phototunable performance was proposed.

2. Experimental

2.1. Reagents

Glucose dehydrogenase (E.C. 1.1.1.47, thermoplasma acidophilum, recombinant expressed in *E. coli*, initial activity of 183 U/mg^{-1}) was obtained from Sigma. NADH was obtained from Beijing Ding Guo Chemical Reagent (Beijing, China). Thionine and branched-poly-ethylenimine (B-PEI) were obtained from Aldrich Chemical Co. They were used as received, without further purification.

Multiwalled carbon nanotubes (MWNTs) (95%, 20–50 nm) purchased from Shenzhen Nanotech. Port. Co. Ltd. (Shenzhen, China) were first shortened and functionalized by sonicating in a mixture of concentrated HNO_3 and H_2SO_4 (v/v, 1:3) for 6 h followed by extensive washing in doubly distilled water until the filtrate was neutral. Then the pH was adjusted to 8.0 to achieved net negatively charged carboxylate groups. The negatively charged MWNTs were centrifuged at 10,000 rpm for 30 min to remove the supernatant and dried in a vacuum. The Au nanoparticles (Au NPs) were prepared by mixing 0.80 mL 1% trisodium citrate, 30 mL of H_2O and 0.3 mL 1% $HAuCl_4$. This solution was kept boiling and stirring 30 min by a magnetic stirring bar at a stirring rate of 500 rpm. Glucose was purchased from Beijing Chemical Reagent (Beijing, China) and the stock solution of glucose was allowed to mutorotate at room temperature overnight before use. 0.1 M phosphate buffer solutions (PBS) consisted of Na_2HPO_4 and NaH_2PO_4 were employed as the supporting electrolyte. All other chemicals were of analytical grade and the solutions were prepared with the doubly distilled water. Urine samples from healthy adults were allowed to precipitate for 15 min at room temperature. The clear upper urine sample was decanted and the remainder discarded. The pH of the urine samples were adjusted to pH 7.5, with 1 M solution of hydrochloric acid or sodium hydroxide as measured by a Delta 320 pH meter (Mettler-Toledo, Shanghai, China).

2.2. Instruments

Cyclic voltammetry and chronamperometry measurements were carried out on a CHI 600 and CHI 832 electrochemical workstation (CH Instruments, USA), respectively. Coiled platinum wire and Ag/AgCl (saturated KCl) electrode were used as the counter electrode and the reference electrode, respectively. Absorption spectra were recorded using a Cary 500 scan UV–vis–NIR spectrophotometer (Varian). The absorbance of multilayer films assembled on quartz slide was measured. Before use, the quartz slide was soaked in freshly prepared "piranha" solution (a mixture of 7:3 volume ratios of 98% H_2SO_4 and 30% H_2O_2) at 90 °C for about 20 min and then washed in pure ethanol and water successively. (*Caution*! "*Piranha*" *solution reacts violently with almost any organic materials and should be handled with extreme care*!). Scanning electron microscopy (SEM) images were determined with a Philips XL-30 ESEM. The accelerating voltage was 20 kV. Photoelectrochemical experiments were performed with the cell irradiated by the white light from Tungsten lamp for 15 min (Spectron, Beijing, L-930), with the light intensity kept at 3.3 mW cm^{-2}.

2.3. Modification of electrodes

Indium-doped tin oxide (ITO) glass plates were cleaned by ultrasonication in a series of solvents, doubly distilled water, ethanol, ethanol aqueous solution saturated by NaOH and ethanol to provide a clean, negative charged surface. The negatively charged substrate ITO was first immersed in B-PEI aqueous solution (2 mg mL^{-1}) with 0.1 M NaCl for 15 min. After being washed with distilled water, the MWNTs/thionine/Au NPs multilayers were grown on the B-PEI-terminated film by alternately dipping the modified ITO electrode into the MWNT solution (0.25 mg mL^{-1}) and thionine aqueous solution (0.1 mM) for 15 min, respectively, and then immersed into AuNPs solution (0.1 mM) and thionine solution for 1 h, respectively. This sequence was repeated until the desired layer number was obtained. The membranes were carefully washed with distilled water. The biosensor for glucose was completed by immersing the $(MWNTs/thionine/AuNPs)_n$ multilayer film modified electrode into the GDH aqueous solution (1 mg/mL, pH 3.0) for 2 h. The amount of GDH was measured spectrophotometrically using Wurster's blue as the electron acceptor essentially as described by Hommes et al. (1984, 1985).

3. Results and discussion

3.1. Characterization of multilayer film

Thionine as a cross-linker to built a MWNTs and AuNPs multilayer has been shown in Scheme 1A. The formation of thionine bridged MWNTs and AuNPs multilayer was confirmed and characterized by SEM image (the inset of Scheme 1A). The sequential repetition of the deposition of MWNTs, thionine and AuNPs could produce a multilayer membrane with a porous structure, which would be favorable for the approach of substrates to the enzyme molecules in internal layers. Further support for the formation of

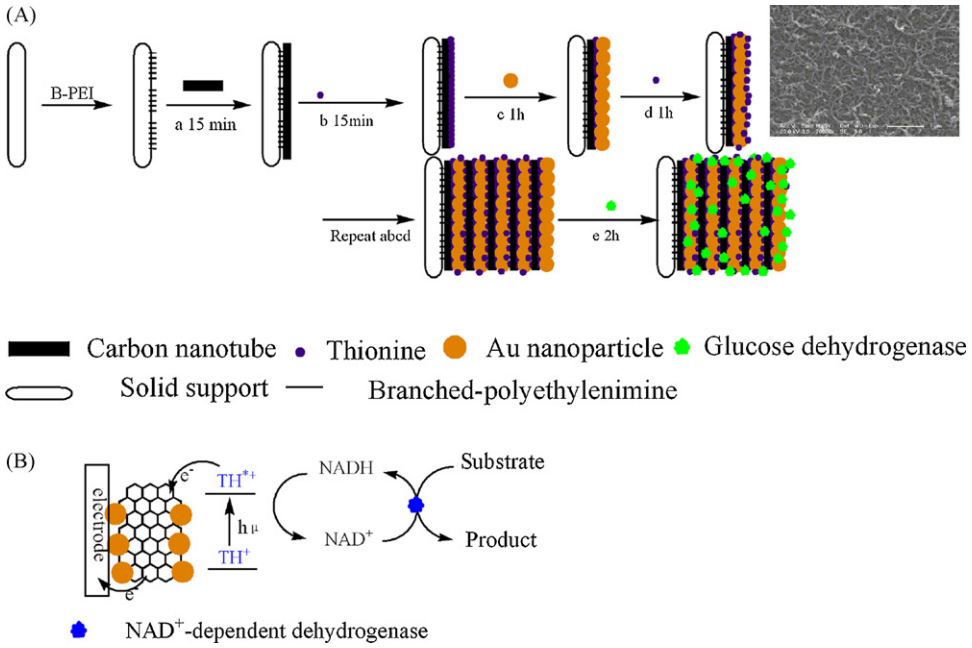

Scheme 1. (A) Schematic structure of the biosensor. Inset: the SEM image of $(MWNTs/thionine/AuNPs)_5$/GDH modified ITO electrode. (B) The reaction scheme of the biosensor under the light irradiation.

$(MWNTs/thionine/AuNPs)_n$ multilayer can be provided by spectroscopy, electrochemistry (data not shown). The absorption band intensities at 267 and 512 nm increased gradually with increasing the number of MWNTs/thionine/AuNPs layer, which could be attributed to the MWNTs and AuNPs, demonstrating that thionine had successfully cross-linked MWNTs and Au NPs into multilayer. The peak currents of thionine in the multilayer and layer numbers exhibited good linear relationship, which implied a linearly growth of the multilayer.

3.2. Detection of NADH at the multilayer modified electrode

Shown in Fig. 1A curve b and x were CVs of the $(MWNTs/thionine/AuNPs)_8$ multilayer modified ITO electrode in PBS (pH 7.0) with and without NADH, respectively. In the presence of NADH, a remarkable catalytic oxidation current at the modified electrode occurred at ca. 30 mV, which shifted 570 mV more negative than that of the bare ITO electrode (ca. 600 mV). The modified electrode gave the best performance for NADH at 8 layers. Thus, the sensor was prepared with eight layers. Self-assembly of MWNTs and AuNPs to electrode surface provided the necessary conduction pathways and allowed efficient electron tunneling, which facilitate electrical communication between NADH and the electrode surface. The oxygen-rich groups such as phenolic hydroxides and quinones presented on the MWNT surface by the acid treatment (Zhang et al., 2004) and the surface bound hydrous oxides of the AuNPs (Jena and Raj, 2006) could function as an efficient mediator. The $(MWNTs/thionine/AuNPs)_n$ films had lots of "cavities" or "channels" to allow counterions to move into or out of the films easily and greatly enhance the charge transport mobility within the films. Such electrocatalytic action facilitated low-potential amperometric measurements of NADH.

It should be mentioned that the above experiments were performed in dark. After the light irradiation on the

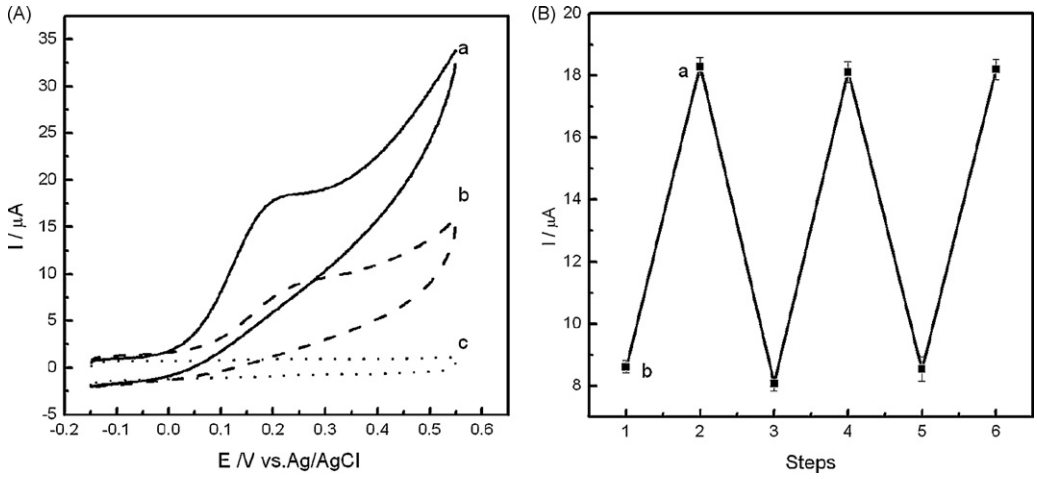

Fig. 1. (A) CVs of the $(MWNTs/thionine/AuNPs)_8$ modified ITO electrodes in pH 7.0 PBS in the absence of NADH in the dark (c) and the in presence of 0.5 mM NADH with (a) and without (b) the light irradiation, respectively. Scan rate: 50 mV s^{-1}. (B) The reversible switch of the current generated by the $(MWNTs/thionine/AuNPs)_8$ modified electrode at 0.2 V with (a) and without (b) light irradiation in pH 7.0 0.1 M PBS containing 0.5 mM NADH.

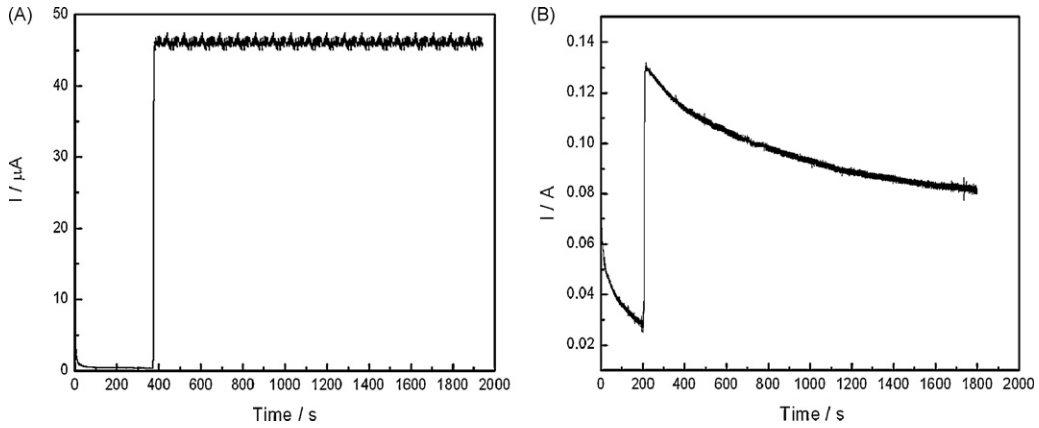

Fig. 2. (A) Response of $(MWNTs/thionine/AuNPs)_8$ multilayer modified ITO electrode at 0.2 V to 2 mM NADH in pH 7.0 0.1 M PBS. (B) Bare ITO electrode at +0.7 V under the same condition in (A).

$(MWNTs/thionine/AuNPs)_8$ films for 15 min, the catalytic current increased significantly in the presence of NADH, in contrast to that in dark. As shown in Fig. 1A curve a, the light irradiation resulted in a negative shifting 50 mV of the anodic peak potential, and the peak current also increased from 8.5 to 18.2 μA. For comparison, the $(MWNTs/AuNPs)_8$ multilayer, the $(MWNTs/thionine)_8$ multilayer and $(AuNPs/thionine)_8$ multilayer modified electrode were prepared according to the reference (Wang et al., 2007b; Huang et al., 2005; Chen et al., 2002). The current at the $(MWNTs/AuNPs)_8$ film modified electrode was no significant difference between the dark and the light irradiation. The light irradiation resulted an obvious enhancement of catalytic current towards NADH at the $(MWNTs/thionine)_8$ multilayer modified electrode. But the current was smaller than that at the $(MWNTs/thionine/AuNPs)_8$ film modified electrode under the same condition. The current at $(AuNPs/thionine)_8$ film modified electrode also exhibited an enhancement with light irradiation. However, the improvement was not as remarkable as that of the $(MWNTs/thionine/AuNPs)_8$ and $(MWNTs/thionine)_8$ film electrode. These phenomena were due to the photovoltaic effect of thionine. Thionine is known to undergo excitation by visible light and a cyclic photochemical reaction with several molecules and ions (Tamilrasan and Natrajan, 1981). Thionine did not have any reaction with NADH in the ground state (Sharma, 1992). So we assumed that MWNTs can serve as electron traps because of the larger electron affinity than the dye (Ikeda and Miyasaka, 2007; Yanagi et al., 2007). Although the AuNPs were reported as the electron acceptor in previous report (Lahav et al., 2000), the worse improvement was observed at the $(AuNPs/thionine)_8$ film than that at those multilayers with the introduction of MWNTs. The MWNTs may act as dominant electron trap in this system. Thionine generated the thionine excited singlet state and triplet state by light absorption and donated an electron to MWNTs. The AuNPs and MWNTs self-assembly provided the necessary conduction pathway and allowed efficient electron transfer to electrode surface. The AuNPs performed an important role in the electron transfer process, since there was worse performance of the multilayer modified electrode without the AuNPs. Then the excited state of thionine was reduced by NADH, which regenerated the photosensitizer and produced NAD^+ (Sharma, 1992). The NAD^+-dependent-dehydrogenase enzyme oxidized substrate, consumed the coenzyme NAD^+ and produced NADH and H^+. The most probable path of the reaction could be summarized in the reaction Scheme 1B. Application of the intermittent light irradiation allowed the selective "ON" and "OFF" switch of the photochemical process. When the thionine was activated by light, the photocatalytical oxidation of NADH should proceed in the system and enhanced the anodic current by 2 folds as compare with that in dark. The interval light irradiation allowed the cyclic activation or inhibition of the photochemical process, and the catalytic performance of the biosensor was tuned between the "low" and "high" states, as shown in Fig. 1B.

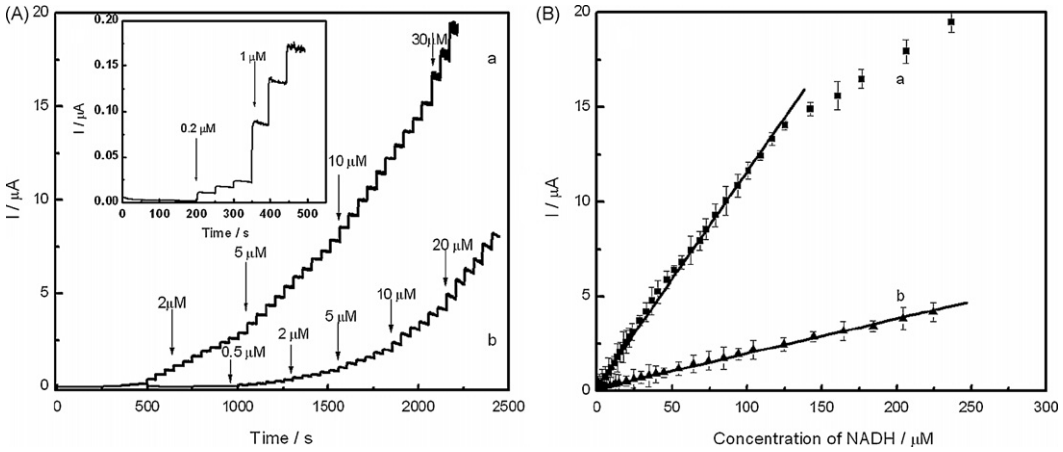

Fig. 3. (A) Amperometric response of the $(MWNTs/thionine/AuNPs)_8$ multilayer modified electrode to the addition of NADH aliquots at 0.2 V into a stirred solution of pH 7.0 0.1 M PBS with (a) and without (b) light irradiation. (B) The corresponding calibration plots.

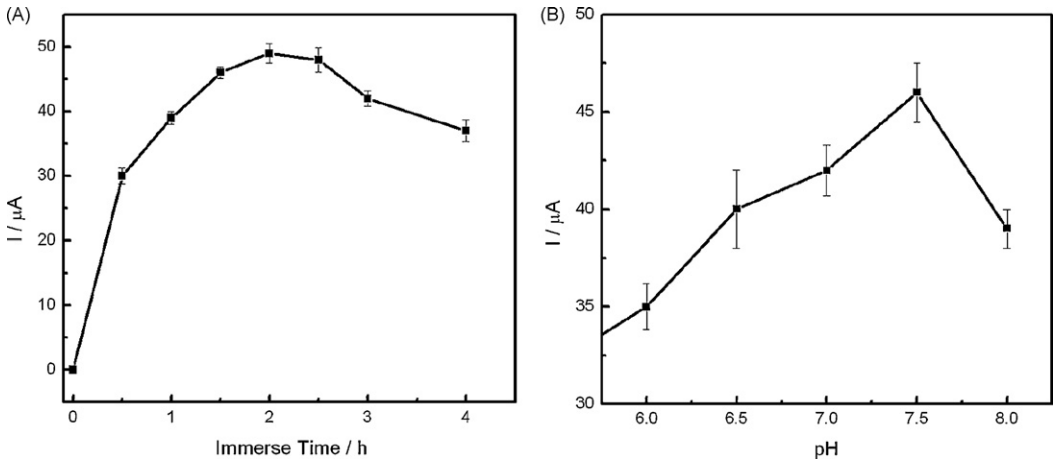

Fig. 4. Effect of immersion time (A) and pH (B) used on the response of the (MWNTs/thionine/AuNPs)$_8$GDH modified electrode in 0.1 M PBS containing 5 mM NADH and 2 mM glucose at 0.2 V under light irradiation.

The voltammetric response of the multilayer modified electrode being left in 2 mM NADH solution for 30 min was decreased 0.3% (Fig. 2A). This demonstrated a resistance of the (MWNTs/thionine/AuNPs)$_n$ film modified electrode to fouling, which was commonly met at other solid electrodes for oxidation of NADH. The better operational stability of the (MWNTs/thionine/AuNPs)$_n$ film modified electrode was due to faster charge transfer and lower overpotential for the oxidation of NADH. The improved kinetics of electron transfer limited the amount of radical intermediates and their dimerization, which typically caused fouling of the electrode surface during the oxidation of NADH via two successive one-electron-transfer steps. Fig. 3A curves a and b showed the amperometric response to the successive addition of NADH in pH 7.0 PBS at the (MWNTs/thionine/AuNPs)$_n$ film modified electrode at +0.20 V under light irradiation and in dark, respectively. The current response displayed a linear range from 0.5 to 237 μM with slope of 17 nA μM^{-1} and detection limit of 0.1 μM in dark. The linear range was from 0.2 to 135 μM with slope of 115 nA μM^{-1} and detection limit of 0.05 μM with the light irradiation. The sensitivity increasing nearly 7 folds and the detection limit lowered 2 folds, in contrast to the catalytic reaction in dark. Taking advantage of the photovoltaic effect of thionine, the (MWNTs/thionine/AuNPs)$_n$ film modified electrodes could catalyze the NADH more efficiently and behave with a higher sensitivity, reactivity and lower detection limit. The electrocatalytic behavior was highly reproducible, as reflected by a relative standard deviation of 4.1% estimated from the slopes of the calibration plots at six freshly prepared (MWNTs/thionine/AuNPs)$_n$ film modified electrodes. When the sensor was not in use, it was stored in pH 7.5 PBS at 4 °C. A decrease of 5.2% amperometric response was observed after 2 months.

3.3. *(MWNT/thionine/AuNPs)$_n$-dehydrogenase-based biosensor for glucose*

The biosensor was prepared by incorporating a model enzyme GDH into the (MWNTs/thionine/AuNPs)$_8$ film. Because of the strong interaction among MWNTs, AuNPs and enzyme, the enzyme can be firmly immobilized in this multilayer structure. The excellent electric property and incompact open structure of (MWNTs/thionine/AuNPs)$_8$ film facilitated the access of substrate and cofactor NAD$^+$ to the GDH and resulted in good catalytic behavior to both NADH and the substrate. The catalytic current of the glucose biosensor depended mainly on the enzyme kinetics which determined the rate at which NADH was generated enzymatically within the multilayer film, and the electrochemical reaction kinetics which controlled the rate at which NADH can be converted to NAD$^+$ to generate the measured electric signal within the (MWNT/thionine/AuNPs)$_8$GDH biocomposite. Therefore, the amount of enzyme immobilized within the biocomposite matrix is crucial for the glucose biosensor sensitivity. The amperometric responses were examined as a function of the time for the modified electrode immersed in GDH solution (Fig. 4A). The glucose biosensor responses enhanced by increasing the immersed time from 30 min to 2 h. The increase was accounted for more enzymatic redox active sites in the (MWNTs/thionine/AuNPs)$_8$GDH biocomposite. The response of the biosensor was reduced after longer immersion time. The abundant GDH within (MWNTs/thionine/AuNPs)$_8$GDH biocomposite disturbed the electron relaying capacity of the (MWNTs/thionine/AuNPs)$_8$ nanostructure due to the insulting GDH. To estimate the amount of the enzyme immobilized on the electrode surface, the residual GDH in solution after modification process was measured spectrophotometrically using Wurster's blue as the electron acceptor essentially as described by Hommes et al. (1984, 1985). So the enzyme loading calculated at the (MWNT/thionine/AuNPs)$_8$ film was 1.25 μg mm^{-2} after 2 h immersed in the enzyme solution. The effect of the concentration of NAD$^+$ on the biosensor response was also investigated with a constant amount of enzyme loading and glucose concentration. The catalytic current for glucose increased with increasing concentration of NAD$^+$ and reached a maximum value at around 5 mM. A further increase in the concentration of NAD$^+$ resulted in a decrease in the catalytic current, probably due to the inhibitory effect of NAD$^+$. Because the enzyme activity is dependent on the pH value of a buffer solution, the effect of pH value of on the current response was examined. A plot of the current responses at (MWNTs/thionine/AuNPs)$_8$GDH biocomposite modified electrode in 0.1 M PBS with different pH values was shown in Fig. 4B. The current response increased by increasing the pH value in the range of 6.0–7.5, and reached a maximum value at pH 7.5. It decreased dramatically at pH above 7.5, which was attributed to the unstability of NAD$^+$ in alkaline solution (Park et al., 1999). Therefore, a solution of pH 7.5 and 5 mM NAD$^+$ in 0.1 M PBS was selected. Fig. 5A showed the steady-state responses of adding different amount of glucose at an applied potential +0.20 V. The response of the sensor was rather fast typically within 10 s. When the biosensor was performed in dark the anodic current increased linearly with the glucose concentration over the range from 10 μM to

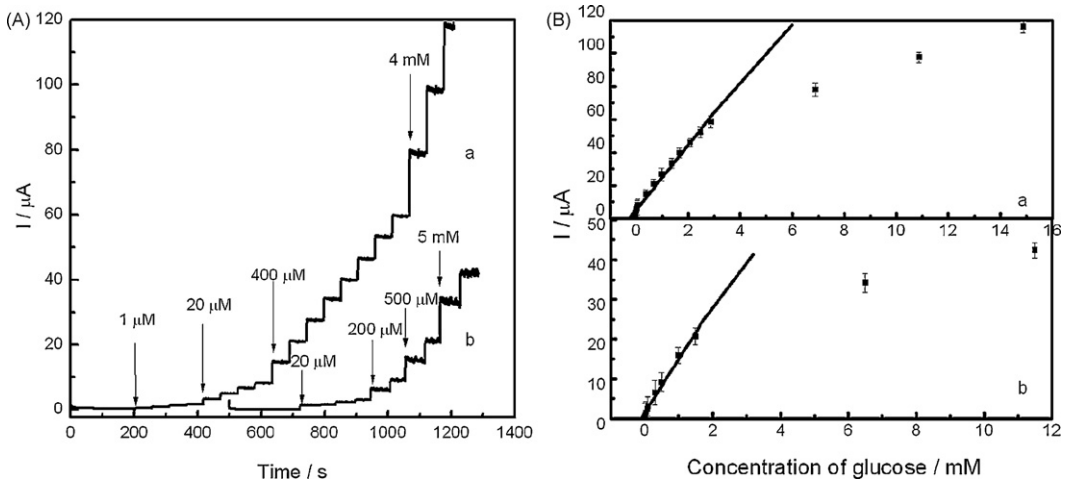

Fig. 5. (A) Amperometric response of the (MWNTs/thionine/AuNPs)$_8$GDH modified electrode to the addition of glucose aliquots at 0.2 V into a stirred solution of 0.1 M pH 7.5 PBS containing 5 mM NADH with (a) and without (b) light irradiation. (B) The corresponding calibration plots.

2.56 mM with the sensitivity of 7.8 μA mM^{-1} and detection limit 5.0 μM. After the light irradiation, the linear range of the biosensor was from 1 μM to 3.25 mM with the sensitivity of 18.5 μA mM^{-1} and detection limit 0.7 μM. The sensitivity increased nearly 2 folds while the detection limit decreased 7 folds, in contrast to the reaction in dark. The photovoltaic effect of the thionine in the multilayer resulted in great enhancement in the electrode's bioelectrocatalytic activity towards NADH and glucose compared to that in dark. The relative standard deviation estimated from the slopes of the calibration plots of six different and freshly prepared glucose sensors was 3.7%, indicating good fabrication reproducibility. The sensor could be repeatedly used for the glucose monitoring. The stability of the (MWNTs/thionine/AuNPs)$_8$GDH modified electrode was investigated when stored in pH 7.5 PBS at 4 °C. After 30 days, the response current was still retained 96% value of the initial response. Response current for continuous usage for 30 days remained 89.2% of the initial response. To assess this biosensor's ability to detect glucose in complex, tainted samples, we tested the (MWNTs/thionine/AuNPs)$_8$GDH modified electrode in the urine. Urine samples were analyzed to evaluate the applicability of the biosensor for glucose analysis. A urine sample collected from a health adult with pH pre-adjustments was used. The standard addition calibrating technique was used for the glucose analysis. The recovery ratios of the four measurements were 95.0%, 103.8%, 98.8% and 96.3%, respectively.

4. Conclusion

The paper represented a dehydrogenase-based electrochemical biosensors with (MWNTs/thionine/AuNPs)$_n$ multilayer. In this structure, the multilayer configuration not only provided a signal transduction of the oxidation of NADH, but also served as a biocompatible scaffold for enzyme immobilization. The photoactive dye cross-linked MWNTs and Au NPs nanostructure allowed the efficient oxidation of NADH, and the biocatalytical performance of the biosensor was greatly improved by the photovoltaic effect of the dye. In contrast to the reaction in dark, the sensitivity increased around 7 folds while the detection limit decreased 2 folds towards NADH with light irradiation. The sensitivity increased over 2 folds and the detection limit lowered 7 folds for glucose compared with that in dark. This indicated possible way to tune the properties of the biosensor for the light-induced performance enhancement and photoswitchable of the biosensor. The MWNTs/dye/AuNPs structure had a potential to provide operational access to a large group of dehydrogenase enzymes, which encompass hundreds of members for designing of a variety of bioelectrochemical devices, e.g. biosensors and biofuel cell.

Acknowledgment

This work was supported by the National Natural Science Foundation of China (Nos. 20575064 and 20675076).

References

Arvinte, A., Valentini, F., Radoi, A., Arduini, F., Tamburri, E., Rotariu, L., Palleschi, G., Bala, C., 2007. Electroanalysis 19, 1455–1459.
Chen, W.L., Jiang, J.G., Dong, S.J., Wang, E.K., 2002. Chem. Commun., 1706–1707.
Curulli, A., Valentini, E., Padeletti, G., Viticoli, A., Caschera, D., Palleschi, G., 2005. Sens. Actuator B: Chem. 111, 441–449.
Deore, B.A., Freund, M.S., 2005. Chem. Mater. 17, 2918–2923.
Hommes, R.W.J., Neijssel, O.M., Tempest, D.W., Dokter, P., Duine, J.A., 1984. Microbiol. Lett. 24, 329–333.
Hommes, R.W.J., van Hell, B., Postma, P.W., Neijssel, O.M., Tempest, D.W., 1985. Arch. Microbiol. 143, 163–168.
Huang, M.H., Jiang, H.Q., Qu, X.H., Xu, Z.A., Wang, Y.L., Dong, S.J., 2005. Chem. Commun., 5560–5562.
Ikeda, N., Miyasaka, T., 2007. Chem. Lett. 36, 466–469.
Jena, B.K., Raj, C.R., 2006. Anal. Chem. 78, 6332–6339.
Katz, E., Lioubashevski, O., Willner, I., 2005. J. Am. Chem. Soc. 127, 3979–3988.
Lahav, M., Heleg-Shabtai, V., Wasserman, J., Katz, E., Willner, I., Dulrr, H., Hu, Y.Z., Bossmann, S.H., 2000. J. Am. Chem. Soc. 122, 11480–11487.
Liu, Y., Wu, S., Ju, H.X., Xu, L., 2007. Electroanalysis 19, 986–992.
Ma, H.Y., Zhang, L.P., Pan, Y., Zhang, K.Y., Zhang, Y.Z., 2008. Electroanalysis 20, 1220–1226.
Maleki, N., Safavi, A., Tajabadi, F., 2006. Anal. Chem. 78, 3820–3826.
Ou, C.F., Yuan, R., Chai, Y.Q., Tang, M.Y., Chai, R., He, X.L., 2007. Anal. Chim. Acta 603, 205–213.
Park, J.K., Yee, H.J., Lee, K.S., Lee, W.Y., Shin, M.C., Kim, T.H., Kim, S.R., 1999. Anal. Chim. Acta 390, 83–91.
Sharma, A., 1992. Spectrochim. Acta 48 (A 6), 893–897.
Tamilrasan, R., Natrajan, P., 1981. Nature 292, 224–225.
Tsai, Y.C., Huang, J.D., Chiu, C.C., 2007. Biosens. Bioelectron. 22, 3051–3056.
Valentini, F., Salis, A., Curulli, A., Palleschi, G., 2004. Anal. Chem. 76, 3244–3248.
Wang, J., Musameh, M., 2003. Anal. Chem. 75, 2075–2079.
Wang, T., Hu, X.G., Dong, S.J., 2007a. J. Mater. Chem. 39, 4189–4195.
Wang, Z.J., Li, M.Y., Zhang, Y.J., Yuan, J.H., Shen, Y.F., Niu, L., Ivaska, A., 2007b. Carbon 45, 2111–2115.
Wu, B.Y., Hou, S.H., Yin, F., Zhao, Z.X., Wang, Y.Y., Wang, X.S., Chen, Q., 2007a. Biosens. Bioelectron. 22, 2854–2860.
Wu, L.N., Zhang, X.J., Ju, H.X., 2007b. Anal. Chem. 79, 453–458.
Yanagi, K., Iakoubovskii, K., Matsui, H., 2007. J. Am. Chem. Soc. 129, 4992–4997.

Yang, M.H., Yang, Y., Yang, H.F., Shen, G.L., Yu, R.Q., 2006. Biomaterials 27, 246–255.
Yu, H.H., Cao, T., Zhou, L.D., Gu, E.D., Yu, D.S., Jiang, D.S., 2006. Sens. Actuator B 119, 512–515.
Zhang, M.G., Gorski, W., 2005. J. Am. Chem. Soc. 127, 2058–2059.
Zhang, M.G., Smith, A., Gorski, W., 2003. Anal. Chem. 75, 2075–2079.
Zhang, M.G., Smith, A., Gorski, W., 2004. Anal. Chem. 76, 5045–5060.
Zhang, M.N., Su, L., Mao, L.Q., 2006. Carbon 44, 276–283.
Zhou, H., Gan, X., Zhu, X.L., Li, G.X., 2005. Anal. Chem. 77, 6102–6104.